1594 *J. Chem. Eng. Data* **2010,** *55,* 1594–1597

Critical Parameters and Saturated Densities in the Critical Region for *trans*-1,3,3,3-Tetrafluoropropene (HFO-1234ze(E))

Yukihiro Higashi* and Katsuyuki Tanaka

Department of Mechanical Systems and Design Engineering, Iwaki Meisei University, 5-5-1, Iino, Chuodai,
Iwaki 970-8551, Japan

Tomohide Ichikawa

Graduate School of Iwaki Meisei University, 5-5-1, Iino, Chuodai, Iwaki 970-8551, Japan

---

Measurements of the saturated vapor and liquid densities near the critical point for *trans*-1,3,3,3-tetrafluoropropene ($CFH{=}CHCF_3$; HFO-1234ze(E)) were carried out in the reduced temperature range of $0.962 < T/T_c < 1$ and in the reduced density range of $0.40 < \rho/\rho_c < 1.70$. Taking into consideration the meniscus disappearing level as well as the intensity of the critical opalescence, the critical temperature T_c and critical density ρ_c were determined experimentally. The critical pressure P_c was calculated by extrapolating the vapor-pressure equation to the critical temperature. The critical parameters reported in this paper are $T_c = (382.51 \pm 0.01)$ K, $\rho_c = (486 \pm 3)$ $kg \cdot m^{-3}$, $V_c = (235 \pm 2)$ $cm^3 \cdot mol^{-1}$, and $P_c = (3632 \pm 3)$ kPa. The saturated liquid density correlation is formulated using the present data. In addition, the critical exponent β along the coexistence curve was also discussed.

Introduction

To prevent the depletion of the ozone layer, hydrofluorocarbons (HFCs) without chlorine and bromine became very popular refrigerants for refrigerators and heat pump systems. Particularly, 1,1,1,2-tetrafluoroethane (HFC-134a) is used as the refrigerant not only for house refrigerators but also for automobile air conditioners. When the European Union's F-gas regulation starts in 2011, new models of automobiles may not be adopt the automobile air-conditioning system with HFCs of global warming potentials (GWPs) greater than 150. Automobile companies all over the world have a serious problem with this change of refrigerants and are searching for new alternative refrigerants with low GWP values.

As with new candidate gases with low GWPs, hydrofluoroolefins (HFOs), for example, HFO-1234yf (2,3,3,3-tetrafluoropropene)[1−3] and HFO-1234ze(E) (*trans*-1,3,3,3-tetrafluoropropene),[4] have lately attracted considerable attention. The advantage of using HFOs is their short atmospheric lifetime. To develop and design the new refrigerating equipment with HFOs, basic information on thermophysical properties and the reliable equation of state are necessary.

In the present paper, the saturated densities of HFO-1234ze(E) along the vapor−liquid coexistence curve near the critical point have been newly measured by visual observation of the meniscus disappearance. On the basis of the present results, the critical temperature and critical density for HFO-1234ze(E) have been determined from the meniscus disappearing level as well as the intensity of the critical opalescence. The critical pressure was calculated from extrapolating the vapor-pressure correlation. In addition, the critical exponent β along the coexistence curve was also discussed for HFO-1234ze(E).

Experimental Section

Chemicals. The sample of *trans*-1,3,3,3-tetrafluoropropene was furnished by Central Glass Co. Ltd., Japan. The manufacturer stated that the sample purity was better than 99.96 % in mole fraction. This sample was used without further purification.

Experimental Apparatus. The measurements of the saturated vapor and liquid densities near the critical point were carried out by the observation of the meniscus disappearance. Despite the fact that the equipment and procedures of measurements have been described in detail in previous papers,[5,6] some information is given below.

The main portion of the apparatus is composed of three high-pressure vessels. The optical cell with two Pyrex windows (15 mm in thickness) is the main vessel in which the change of the meniscus behavior of the sample mixture can be observed. The cylindrical body of this optical cell was made of 304 stainless steel (50 mm in length, (16 to 18) mm in inner diameter, and 11.620 cm^3 in inner volume at room temperature). The inner shape of this optical cell is barrel-shaped to make it easier to observe the phenomenon of meniscus disappearance. The expansion vessel (8.949 cm^3 in inner volume at room temperature) and supplying vessel (77.575 cm^3 in inner volume at room temperature) are the cylindrical vessels made of 304 stainless steel and are used to change the sample density in the optical cell without a new sample charge.

The apparatus was installed in a thermostatted silicone oil bath. The bath temperature can be kept constant within a temperature fluctuation of ± 5 mK with two electric heaters of 1.5 kW and 300 W. The temperature measurement was conducted by a 25 Ω standard platinum resistance thermometer (Chino, model: R800-2) calibrated against ITS-90 with the aid of a thermometer bridge (Automatic Systems Laboratories, model: F700). The thermometer was mounted in the vicinity of the optical cell. The uncertainty of temperature measurements

---

* Corresponding author. E-mail address: higashi@iwakimu.ac.jp.

10.1021/je900696z

Table 1. Experimental Saturated Densities near the Critical Point of *trans*-1,3,3,3-Tetrafluoropropene[a]

T K	ρ $\text{kg}\cdot\text{m}^{-3}$
368.798	193.7 ± 1.0
370.705	208.0 ± 1.2
372.223	223.2 ± 1.2
373.954	238.8 ± 1.2
376.500	263.1 ± 1.4
377.289	270.9 ± 1.0
379.134	290.9 ± 1.3
379.775	312.2 ± 1.2
380.502	334.0 ± 1.2
371.078	342.6 ± 1.0
381.648	368.0 ± 1.4
382.079	394.9 ± 1.2
382.350	422.6 ± 1.3*
382.510	479.4 ± 0.7*
382.513	485.9 ± 0.5*
382.504	514.9 ± 1.1*
382.404	552.5 ± 0.8*
382.053	591.3 ± 0.9*
381.678	606.5 ± 0.5
380.568	651.5 ± 1.0
378.416	699.2 ± 0.6
375.337	748.3 ± 0.7
368.204	824.7 ± 0.7

[a] Critical opalescence was observed at the data point with an asterisk.

was estimated to be within ± 10 mK. The sample density was calculated from the sample mass and the inner volumes of the pressure vessels by using expansion procedures. The uncertainty of the density measurement changes in proportion to the amount of expansion. The uncertainties of the density measurements were estimated to be within (0.5 to 1.4) $\text{kg}\cdot\text{m}^{-3}$.

Results and Discussion

Measurements of the Saturated Densities near the Critical Point for HFO-1234ze(E). The saturated vapor and liquid densities near the critical point for HFO-1234ze(E) were measured by the observation of the meniscus disappearance. The experimental data of saturated vapor and liquid densities are summarized in Table 1. Fourteen data of saturated vapor densities, eight data of saturated liquid densities, and one datum in the very vicinity of the critical point, which is undistinguishable as to whether it is saturated liquid or saturated vapor, were obtained in the temperature range from 368.204 K to the critical temperature and in the density range between (193.7 and 824.7) $\text{kg}\cdot\text{m}^{-3}$. This range of measurement corresponds to the reduced temperature range of $0.962 < T/T_c < 1$ and to the reduced density range of $0.399 < \rho/\rho_c < 1.697$, respectively.

Figure 1 shows the vapor−liquid coexistence curve near the critical point for HFO-1234ze(E) on temperature−density plane. For the saturated liquid density, Grebenkov et al.[4] have recently reported the experimental data in the wide temperature range from (251 to 380) K. No other experimental data for the saturated liquid densities as well as the saturated vapor densities near the critical point can be found up to the present.

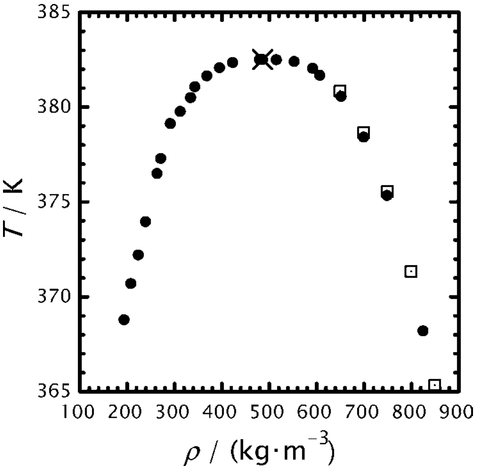

Figure 1. Vapor−liquid coexistence curve near the critical point for HFO-1234ze(E). ●, present work; ⊡, Grebenkov et al.;[4] ×, critical point.

Determination of the Critical Temperature and Critical Density for HFO-1234ze(E). The critical opalescence was observed at six data points marked with an asterisk in Table 1 in the density range from (422.6 to 591.3) $\text{kg}\cdot\text{m}^{-3}$. The meniscus at the density of 422.6 $\text{kg}\cdot\text{m}^{-3}$ was located at the center level in the optical cell when the temperature was the room temperature. With increasing temperature, the meniscus level gradually descended and disappeared at the bottom of the optical cell. At this density, the critical opalescence was observed only in the liquid phase. The meniscus at the density of 479.4 $\text{kg}\cdot\text{m}^{-3}$ was located at the center level in the optical cell when the temperature was the room temperature. With increasing temperature, the meniscus level slightly descended but disappeared prior to reaching the bottom of the optical cell. At this density, the critical opalescence was observed in the both phases of liquid and vapor. Moreover, the intensity of the critical opalescence in the liquid phase was observed to be stronger than that in the vapor phase. This density of 479.4 $\text{kg}\cdot\text{m}^{-3}$ was considered to be at a condition that was slightly lower than the critical density.

The meniscus at the densities of (552.5 and 591.3) $\text{kg}\cdot\text{m}^{-3}$ was located at the center level in the optical cell when the temperature was the room temperature. With increasing temperature, the meniscus level gradually ascended and disappeared at the top of the optical cell. At this density, the critical opalescence was not observed in the liquid phase but was observed in the vapor phase. The meniscus at the density of 514.9 $\text{kg}\cdot\text{m}^{-3}$ was located at the center level in the optical cell when the temperature was the room temperature. With increasing temperature, the meniscus level gradually ascended but disappeared prior to reaching the top of the optical cell. At this density, the intensity of the critical opalescence in the vapor phase was observed to be stronger than that in the liquid phase. These three densities from (514.9 to 591.3) $\text{kg}\cdot\text{m}^{-3}$ were considered to be at a condition that was slightly higher than the critical density.

The meniscus at the density of 485.9 $\text{kg}\cdot\text{m}^{-3}$ was located at the center level in the optical cell when the temperature was the room temperature. The meniscus level was unchanged at the center in the optical cell with increasing temperature and finally disappeared at the center level. The intensity of the critical opalescence in the vapor phase was almost same as that in the liquid phase. Moreover, the meniscus reappearance level was located at the center level. As the result of exact observation, the density of 485.9 $\text{kg}\cdot\text{m}^{-3}$ was considered to be very close to the critical density.

On the basis of these observations of meniscus disappearance, the critical temperature T_c and the critical density ρ_c for HFO-1234ze(E) were experimentally determined as:

$$T_c = (382.51 \pm 0.01)\ \text{K} \tag{1}$$

$$\rho_c = (486 \pm 3)\ \text{kg}\cdot\text{m}^{-3} \tag{2}$$

The critical molar volume V_c was converted from the critical density using the molar mass of HFO-1234ze(E),[7] $M = 114.0416\ \text{g}\cdot\text{mol}^{-1}$.

$$V_c = (235 \pm 2)\ \mathrm{cm^3 \cdot mol^{-1}} \tag{3}$$

Critical Pressure for HFO-1234ze(E). The critical pressure P_c can be calculated from the extrapolation of the vapor-pressure correlation with the aid of the T_c value. With respect to the vapor-pressure correlation for HFO-1234ze(E), the following correlation formulated by Tanaka et al.[8] has been adopted. The functional form of the vapor-pressure correlation is the same as that for HFO-1234yf.[2]

$$\ln\left(\frac{P}{P_c}\right) = \frac{T_c}{T}(A_1\tau + A_2\tau^{1.5} + A_3\tau^{2.5} + A_4\tau^5) \tag{4}$$

In eq 4, T_c and P_c denote the critical temperature and critical pressure, respectively. The reduced temperature difference τ means $1 - T/T_c$. Coefficients A_1 to A_4 in eq 4 are summarized in Table 2.

The critical pressure for HFO-1234ze(E) calculated as the extrapolating value to the critical temperature of 382.51 K was 3632 kPa. The uncertainty of the critical pressure depends upon the uncertainty of the critical temperature and the accuracy of the vapor-pressure correlation. Taking into consideration these factors, the critical pressure for HFO-1234ze(E) was determined finally as follows:

$$P_c = (3632 \pm 3)\ \mathrm{kPa} \tag{5}$$

The critical temperature reported by Grebenkov et al., T_c = 382.75 ± 0.2 K, seems to be higher than the present critical temperature, 0.24 K. Taking into consideration their claimed uncertainty of T_c to be 0.2 K, both T_c values agree with one another. As for the critical pressure, the reported P_c value by Grebenkov et al. of 3681 kPa is 49 kPa higher than the present critical pressure. Grebenkov et al. also determined the critical pressure by extrapolating the vapor-pressure correlation to the critical temperature. If the higher critical temperature value is used for the extrapolation, the calculated critical pressure becomes higher. The critical density value could not be compared because there is no experimental data available on the reported literature.

Saturated Liquid-Density Correlation. By using not only the saturated liquid-density data in the present work but also those reported by Grebenkov et al.,[4] a new saturated liquid-density correlation for HFO-1234ze(E) is formulated. The functional form of the saturated liquid-density correlation is adopted as follows.

$$\frac{\rho}{\rho_c} = 1 + C_1\tau^{1/3} + C_2\tau^{2/3} + C_3\tau + C_4\tau^{4/3} + C_5\tau^3 \tag{6}$$

where $\tau = 1 - T/T_c$. By least-squares fit, coefficients C_1 to C_5 in eq 6 are determined and summarized in Table 3. The deviation plot between the experimental data and this correlation is shown in Figure 2. The effective temperature range of this correlation is between 250 K and critical temperature, although the reproducibility of the experimental data becomes worse near the critical point. The standard deviation and average deviation of all experimental data between 250 K and critical temperature are 0.34 % and 0.24 %, respectively. In the case of the effective temperature range between (250 and 380) K except for the vicinity of the critical point, the standard deviation and average deviation of this correlation improve by 0.24 % and 0.19 %, respectively.

Table 2. Coefficients of the Vapor-Pressure Correlation in Equation 4

T_c / K	P_c / kPa	A_1	A_2	A_3	A_4
382.51	3632	–7.60109	2.00169	–3.85312	21.2611

Table 3. Coefficients of the Saturated Liquid-Density Correlation in Equation 6

T_c / K	ρ_c / kg·m^{-3}	C_1	C_2	C_3	C_4	C_5
382.51	486	2.08011	–1.33802	5.87549	–5.33744	3.55692

Critical Exponent β. The critical exponent β along the coexistence curve can be determined on the basis of the power law representations.

$$|(\rho - \rho_c)/\rho_c| = B\tau^\beta \tag{7}$$

where $\tau = 1 - T/T_c$ is the reduced temperature difference. Coefficient B and exponent β stand for the critical amplitude and the critical exponent along the coexistence curve, respectively.

The relation between $\log|(\rho - \rho_c)/\rho_c|$ and $\log \tau$ in eq 7 is presented in Figure 3. The power law representation by eq 7 suggests that the experimental results may be fitted by a straight line with a gradient equivalent to the critical exponent β. Thirteen saturated vapor-density data and seven saturated liquid-

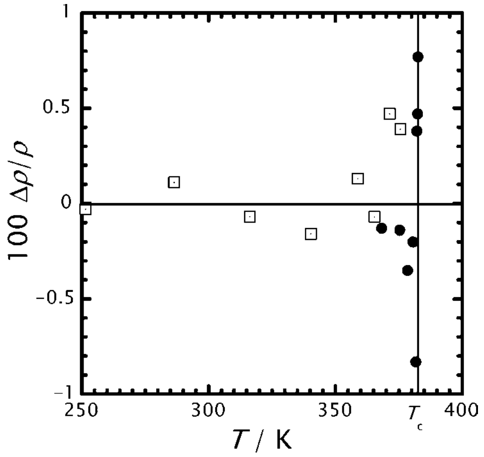

Figure 2. Fractional deviations $\Delta\rho = \rho_{calc} - \rho_{expt}$ of the experimental saturated densities ρ_{expt} against eq 6. ●, present work; ⊡, Grebenkov et al.[4]

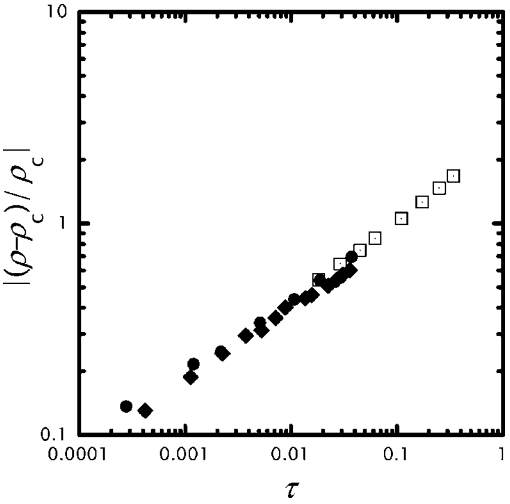

Figure 3. Relationship between the reduced density difference and the reduced temperature difference. ●, present work (saturated liquid); ◆, present work (saturated vapor); ⊡, Grebenkov et al.[4] (saturated liquid).

density data except three data, that is, (479.4, 485.9, and 514.9) kg·m^{-3}, in the very vicinity of the critical point were used to determine the critical amplitude B and critical exponent β by the least-squares fit. The values of B and β determined in this work are 2.005 and 0.332 for the saturated liquid and 1.878 and 0.338 for the saturated vapor, respectively. The obtained values of critical exponent β for the saturated liquid and vapor are greater than the theoretical value of 0.326 but are in good agreement with the reported β values by the present authors.[9,10]

Acknowledgment

The authors are grateful to Central Glass Co. Ltd., Japan, for furnishing the sample and analyzing the purity of the sample.

Literature Cited

(1) Minor, B. H.; Spartz, M. A. In *Evaluation of HFO-1234yf for Mobile Air Conditioning*. Proceedings of 2008 SAE World Congress, Detroit, MI, 2008.
(2) Tanaka, K.; Higashi, Y. Thermodynamic Properties of HFO-1234yf(2,3,3,3-tetrafluoropropene). *Int. J. Refrig.*, in press.
(3) Nicola, G. D.; Polonara, F.; Santori, G. Saturated Pressure Measurements of 2,3,3,3-tetrafluoroprop-1-ene (HFO-1234yf). *J. Chem. Eng. Data*, DOI: 10.021/je900306v.
(4) Grebenkov, A. J.; Hulse, R.; Pham, H.; Singh, R. In *Physical Properties and Equation of State for Trans-1,3,3,3-Tetrafluoropropene*. Proceedings of 3rd IIR Conference on Thermophysical Properties and Transfer Processes of Refrigerants, Boulder, CO, 2009; paper no. 191.
(5) Okazaki, S.; Higashi, Y.; Takaishi, Y.; Uematsu, M.; Watanabe, K. Procedures for Determining the Critical Parameters of Fluids. *Rev. Sci. Instrum.* **1983**, *54*, 21–25.
(6) Higashi, Y.; Okazaki, S.; Takaishi, Y.; Uematsu, M.; Watanabe, K. Measurements of the Vapor-Liquid Coexistence Curve for the Binary R12 + R22 System in the Critical Region. *J. Chem. Eng. Data* **1984**, *29*, 31–36.
(7) Wieser, M. E. Atomic Weights of the Elements 2005. (IUPAC Technical Report). *Pure Appl. Chem.* **2006**, *78*, 2051–2066.
(8) Tanaka, K.; Takahashi, G.; Higashi, Y. Measurements of the Vapor Pressures and PρT Properties for trans-1,3,3,3-tetrafluoropropene. *J. Chem. Eng. Data*, submitted.
(9) Higashi, Y.; Uematsu, M.; Watanabe, K. Determination of the Vapor-Liquid Coexistence Curve and the Critical Parameters for Refrigerant 502. *Int. J. Thermophys.* **1984**, *5*, 117–129.
(10) Higashi, Y.; Ikeda, T. Critical Parameters for 1,1,1-trifluoroethane (R-143a). *Fluid Phase Equilib.* **1996**, *125*, 139–147.

Received for review August 21, 2009. Accepted December 16, 2009.

JE900696Z